Transport properties of nanosystems with conventional and unconventional charge density waves

Marcin Mierzejewski and Maciej M. Maśka

Department of Theoretical Physics, Institute of Physics, University of Silesia, 40-007 Katowice, Poland

We report a systematic study of transport properties of nanosytems with charge density waves. We demonstrate how the presence of density waves modifies the current-voltage characteristics. On the other hand, we show that the density waves themselves are strongly affected by the applied voltage. This self-consistent problem is solved within the formalism of the nonequilibrium Green's functions. The conventional charge density waves occur only for specific, periodically distributed ranges of the voltage. Apart from the low-voltage regime, they are incommensurate and the corresponding wave vectors decrease discontinuously when the voltage increases.

I. INTRODUCTION

Transport properties of nanosystems are very different from those of macroscopic conductors. In particular, nonlinear or even irregular current-voltage characteristics seem to be intrinsic properties of these systems. Although a great number of theoretical and experimental results concern quantum dots, there is an increasing interest in the transport properties of nanowires and single molecules.[1–4] The main reason for such a tendency is their possible application in future electronic devices. Theoretical analysis of the transport phenomena is difficult due to the coupling between the nanosystem and macroscopic leads. As a consequence, Coulomb correlations are usually taken into account only approximately.

The spatial confinement that originates from the geometry of the nanosystem may be responsible for inhomogeneity of the charge distribution. Additionally, one may expect that phenomena typical for low-dimensional correlated systems, e.g., charge density waves (CDWs), occur as well. Most of the research on the conductance of low-dimensional systems with CDW correlations focuses on sliding density waves.[5–7] This transport mechanism sets in for incommensurate CDWs when the applied voltage exceeds the depinning threshold. For finite incommensurate CDW systems it has been shown that the transport properties are controlled predominantly by the leads.[8] It has also been shown that the conductance of a commensurate CDW system is very different from that of an incommensurate one. The theoretical description of incommensurate CDWs is similar to the theory of the Luttinger liquid. The resulting temperature dependence of the conductance is much simpler than that of commensurate CDWs.[9] These results lead straightforwardly to a question about the mechanisms that determine the commensurability of CDWs in meso- and nanoscales, e.g, whether commensurability of the charge distribution depends on the bias voltage and the geometry of the nanosystem. Recent self-consistent investigations of the molecular chain show that the charge distribution strongly depends on the applied voltage.[10,11] This effect has already been observed in molecular devices.[1,12] In analogy to this result, one may expect that the applied voltage changes also the charge distribution in the CDW system, which affects the current-voltage characteristic. The current itself can modify the charge distribution as well. As a result,

we may obtain a system, where small changes of the applied voltage can, through the modification of the charge distribution, drive the system between insulating and metallic states. It is possible, that this tempting feature of the CDW nanosystems could be applied in switching devices.

In the present paper we use the formalism of nonequilibrium Green's functions to analyze the charge distribution in a nanosystem coupled to leads. We demonstrate that the applied voltage can induce a transition between commensurate and incommensurate CDWs. We analyze how this transition depends on the geometry of the nanosystem. The transport properties determined for conventional CDWs are compared with the results obtained for systems with unconventional density waves.[13] In particular, we analyze density wave states with *d*-wave symmetry (DDWs) that have been intensively investigated as a possible scenario for the pseudogap phase in high-temperature superconductors.[14] Such an order has also been proposed as the low-temperature phase of some quasi-two-dimensional organic conductors.[16]

II. MODEL AND METHOD

The Hamiltonian of the system under consideration consists of three parts which describe the nanosystem itself, macroscopic electrodes and the coupling between the electrodes and the nanosystem: $H = H_{\text{nano}} + H_{\text{el}} + H_{\text{nano-el}}$. The electrodes are modeled by a lattice gas of noninteracting electrons with a wide energy band: $H_{\text{el}} = \sum_{\mathbf{k},\sigma,\alpha} (\varepsilon_{\mathbf{k},\alpha} - \mu_{\alpha}) c^{\dagger}_{\mathbf{k},\sigma,\alpha} c_{\mathbf{k},\sigma,\alpha}$, where μ denotes the chemical potential and $\alpha \in \{L, R\}$ indicates the left or right electrode. $c^{\dagger}_{\mathbf{k},\sigma,\alpha}$ creates an electron with momentum $\mathbf{k}$ and spin σ in the electrode α. At the mean-field level the Hamiltonian of the nanosystem is given by

$$H_{\text{nano}} = \sum_{\langle ij \rangle \sigma} [-t_{ij} + (-1)^i U_{\text{DDW}} W_{ij}] c^{\dagger}_{i\sigma} c_{j\sigma}$$

$$- U_{\text{CDW}} \sum_{i\sigma} \left(\langle n_{i-\sigma} \rangle - \frac{1}{2} \right) c^{\dagger}_{i\sigma} c_{i\sigma}, \qquad (1)$$

where $c^{\dagger}_{i\sigma}$ creates an electron with spin σ at site i of the nanosystem, $n_{i\sigma} = c^{\dagger}_{i\sigma} c_{i\sigma}$, and $W_{ij} = (-1)^i \langle c^{\dagger}_{i\sigma} c_{j\sigma} - c^{\dagger}_{j\sigma} c_{i\sigma} \rangle / 2$.

205103-1

The potentials U_{CDW} and U_{DDW} describe the strengths of interactions that are responsible for the formation of conventional and unconventional charge density waves, respectively.[15,17] The coupling between the nanosystem and the electrodes is described by

$$H_{\text{nano-el}} = \sum_{\mathbf{k},i,\alpha,\sigma} (g_{\mathbf{k},i,\alpha} c^{\dagger}_{\mathbf{k},\sigma,\alpha} c_{i\sigma} + \text{H.c.}). \qquad (2)$$

A few remarks concerning the validity of the mean-field approach are needed at this stage. It is generally believed that the mean-field approximation is inappropriate for low-dimensional systems. However, it has been argued that this approximation may be applicable at low temperatures for weak interaction and strong coupling between the nanosystem and electrodes (see Ref. 10 and the discussion therein). Therefore, we restrict our considerations to the case $U_{\text{CDW(DDW)}} < 4t$ and assume a relatively strong coupling between the electrodes and the nanosystem. Additionally, the recent investigations of nanorings with CDW correlations have shown that the mean-field results qualitatively agree with the exact ones[18] (although the quantitative differences remain significant). These results concern the properties of persistent currents in a system where the CDW is pinned by impurities. In the present case, the coupling to electrodes should play a similar role in stabilizing the CDW. Consequently, we expect that the mean-field analysis provides correct qualitative results for the transport currents in a CDW system.

The thermal averages that occur in the Hamiltonian (1) are calculated self-consistently using the lesser Keldysh Green's functions

$$\langle c^{\dagger}_{i\sigma} c_{j\sigma} \rangle = \frac{1}{2\pi i} \int d\omega G^{<}_{j\sigma,i\sigma}(\omega). \qquad (3)$$

After obtaining convergency, one can calculate the current flowing through the nanosystem,

$$J = \frac{2e}{h} \int d\omega [f_L(\omega) - f_R(\omega)] \text{Tr}[\hat{\Gamma}_L(\omega) \hat{G}^r(\omega) \hat{\Gamma}_R(\omega) \hat{G}^a(\omega)], \qquad (4)$$

where $f_\alpha(\omega)$ is the Fermi function of electrons in the electrode α. The elements of the matrix $\hat{\Gamma}_{L(R)}$ are given by

$$[\hat{\Gamma}_\alpha(\omega)]_{ij} = 2\pi \sum_{\mathbf{k}} g^{*}_{\mathbf{k},i,\alpha} g_{\mathbf{k},j,\alpha} \delta(\omega - \varepsilon_{\mathbf{k},\alpha}), \qquad (5)$$

whereas the matrices $\hat{G}^r(\omega)$ and $\hat{G}^a(\omega)$ consist of retarded and advanced Keldysh Green's functions, respectively. For the sake of brevity we do not present the complete set of equations that determine the Green's functions for the mean-field Hamiltonian. Instead we refer to Ref. 10 for the details.

III. CONVENTIONAL CHARGE DENSITY WAVES

We start our investigations with a one-dimensional (1D) nanowire taking into account only the nearest-neighbor hopping. The ends of the nanowire are connected to the macro-

scopic leads. The only nonvanishing elements of the $\hat{\Gamma}$'s are assumed to be frequency independent $[\hat{\Gamma}_L(\omega)]_{11} = [\hat{\Gamma}_R(\omega)]_{NN} = \Gamma$, where the sites in the chain are enumerated from 1 to N. The difference between the lead's potentials gives the voltage applied to the nanosystem, $eV = \mu_L - \mu_R$.

In a 1D system a d density wave cannot occur and, therefore, in this case we restrict ourselves only to the conventional charge density wave ($U_{\text{DDW}} = 0$). Figure 1 shows current-voltage (*I-V*) characteristics of 20- and 40-atom chains coupled to the macroscopic leads. Here, we compare the characteristics obtained for $U_{\text{CDW}} = 1.5t$ with the results for a noninteracting system ($U_{\text{CDW}} = 0$).

In the uncorrelated case the *I-V* characteristic consists of a series of plateaus smoothly connected by steep sections. In the following, we refer to these plateaus as *original plateaus*. In the presence of the CDW interaction additional smaller plateaus occur instead of these steep sections and the resulting *I-V* characteristic changes from a relatively smooth one to a step function. Within the original plateaus the characteristic remains almost unchanged. These results clearly show that the CDW correlations modify the *I-V* characteristic only for some particular values of *V*. It occurs as a result of a strong suppression of the charge density waves by the applied voltage in the regions of the original plateaus. In order to confirm this statement we have analyzed the spatial distribution of electrons over the nanowire. Figure 2 shows the occupation number as a function of position for a 20-atom chain at various voltages. We have found that within the original plateaus electrons are distributed almost uniformly over the system. Contrary to this, in the regions where the additional plateaus occur the electron density is strongly inhomogeneous and can be described as (in most cases incommensurate) charge density waves, i.e., $\langle n_{i\sigma} \rangle$ can be fitted very accurately by $n^0 + A \cos(\mathbf{Q} \cdot \mathbf{R}_i + \phi)$. It turns out that the CDW wave vector $\mathbf{Q}$ strongly depends on *V*. For $V = 0$ the CDW is commensurate with the lattice ($|\mathbf{Q}| = \pi$). The same holds true for a small voltage. However, when the voltage increases, the CDW wavelength increases as well. Figure 3 shows how the density wave vector $\mathbf{Q}$ and and the density wave amplitude A change with the applied voltage. Similarly to the *I-V* characteristic $\mathbf{Q}(V)$ is a step function, whereas $A(V)$ is approximately a two-value periodic function. Comparing Figs. 1 and 3 one can see that each of the additional plateaus in the *I-V* characteristic corresponds to a different value of the CDW wave vector. The overall behavior of the *I-V* and $\mathbf{Q}(V)$ characteristics obtained for the 20-atom chain is similar to those obtained for the 40-atom wire. The main difference is related to the number and length of the plateaus; namely, the number of allowed values of $\mathbf{Q}$ increases with increasing length of the nanowire. Moreover, the ratio of the lengths of the original and CDW-induced plateaus decreases when the length of the nanowire increases. It suggests that for a sufficiently long nanowire $\mathbf{Q}$ should become a continuously decreasing function of *V*. Comparison of Figs. 3(a) and 3(b) illustrates this tendency. In an isolated 1D system the CDW wave vector can be changed by the modification of the Fermi wave vector ($|\mathbf{Q}| = 2k_F$), which in turn is a single-valued function of the occupation number. In the present case $\mathbf{Q}$ can be changed independently of the concentration of electrons by means of the applied voltage.
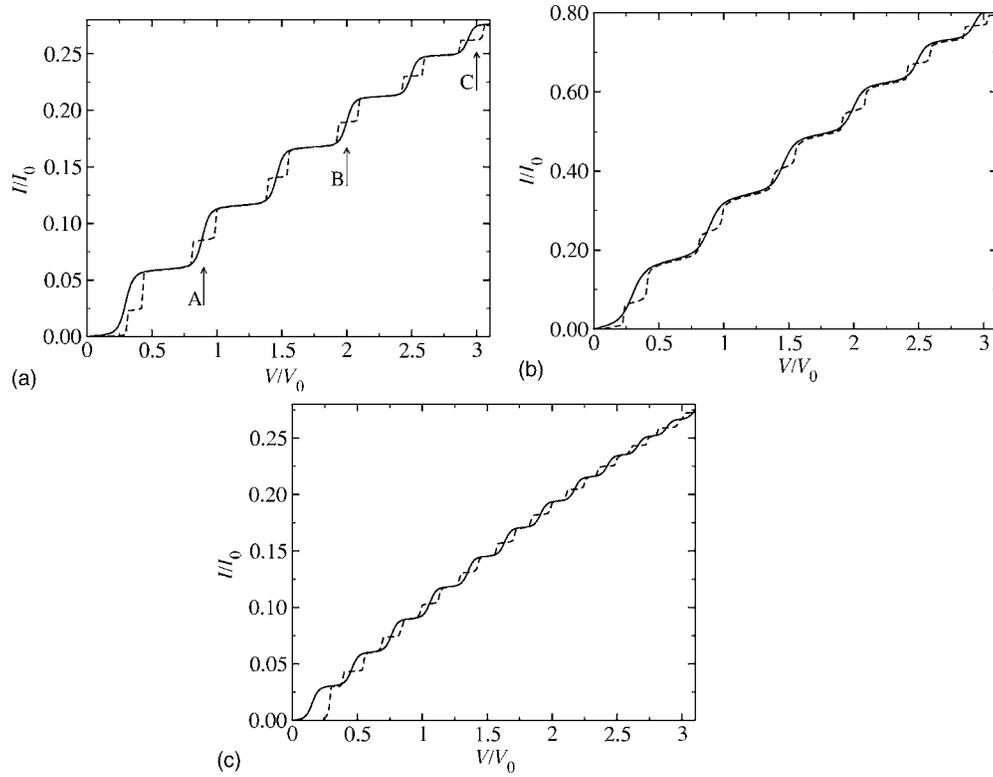
FIG. 1. Current-voltage characteristics of one-dimensional chains containing 20 [(a) and (b)] and 40 (c) atoms for the temperature of the leads $k_B T = 0.01t$. (a) and (c) correspond to $\Gamma = 0.1t$ and (b) to $\Gamma = 0.3t$. Continuous and dashed lines show results obtained for $U_{CDW} = 0$ and $U_{CDW} = 1.5t$, respectively. We have denoted $I_0 = 2et/h$ and $V_0 = t/e$, where t is the nearest-neighbor hopping integral (Ref. 19). Arrows labeled as A, B, and C indicate voltages for which the charge distributions are shown in Fig. 2.

In order to get insight into the physical origin of the above results, one can consider an isolated chain. In this case, the onset of the charge density waves is determined by the CDW susceptibility, defined as a retarded equilibrium Green's function:
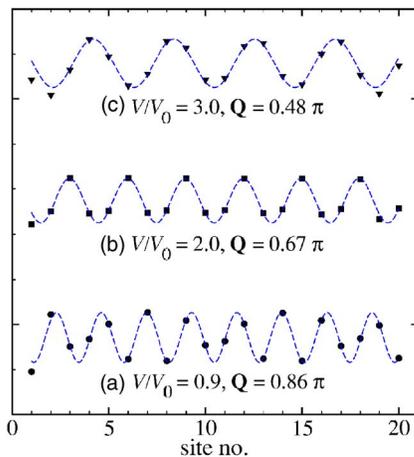
FIG. 2. (Color online) Average occupation $\langle n_{i\sigma} \rangle$ obtained for a 20-atom chain with $U_{CDW} = 1.5t$ The voltage is indicated explicitly in the figure, whereas the remaining model parameters are the same as in Fig. 1. Results have been fitted by the function $\langle n_{i\sigma} \rangle = n^0 + A \cos(\mathbf{Q} \cdot \mathbf{R}_i + \phi)$. For clarity of the figure the curves are offset.
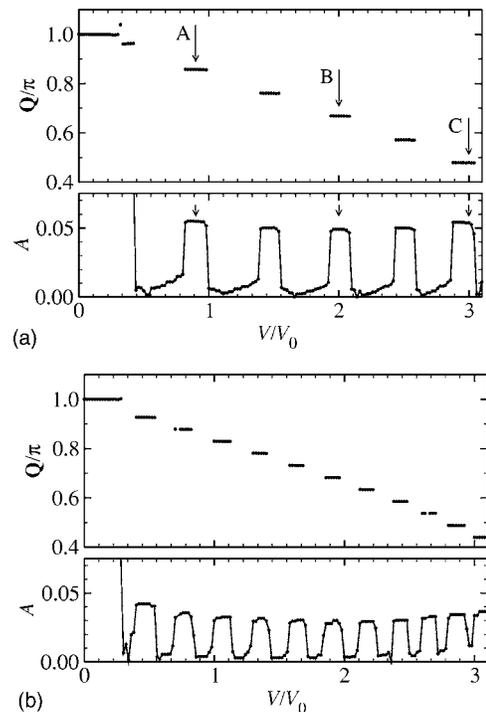
FIG. 3. Voltage dependence of the density wave amplitude A and the wave vector $\mathbf{Q}$ for chains containing 20 (upper panel) and 40 (lower panel) atoms. Model parameters are the same as in Fig. 1. Arrows labeled as A, B, and C denote cases presented in Fig. 2.
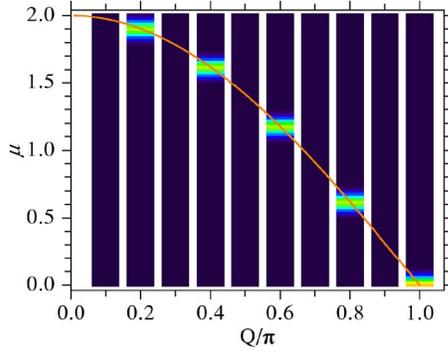
FIG. 4. (Color online) CDW susceptibility as a function of the chemical potential μ and the wave vector $\mathbf{Q}$. Lighter regions correspond to larger values of the susceptibility. These results have been obtained for an isolated 20-atom chain with the nearest-neighbor hopping and periodic boundary conditions. The solid line shows $\mu=2t\cos(|\mathbf{Q}|/2)$ (see text for explanation).

$$\chi(\mathbf{Q},\omega) = -\langle\langle\hat{\Delta}(\mathbf{Q})|\hat{\Delta}^{\dagger}(\mathbf{Q})\rangle\rangle, \quad (6)$$

where

$$\hat{\Delta}(\mathbf{Q}) = \frac{1}{N}\sum_{\mathbf{k},\sigma} c^{\dagger}_{\mathbf{k}+\mathbf{Q},\sigma} c_{\mathbf{k},\sigma}, \quad (7)$$

and $c^{\dagger}_{\mathbf{k},\sigma}$ creates an electron with momentum $\mathbf{k}$ and spin σ. In the static case, the CDW susceptibility is given by the Lindhard function:

$$\chi(\mathbf{Q},\omega=0) = \frac{2}{N}\sum_{\mathbf{k}}\frac{f(\epsilon_{\mathbf{k}+\mathbf{Q}})-f(\epsilon_{\mathbf{k}})}{\epsilon_{\mathbf{k}+\mathbf{Q}}-\epsilon_{\mathbf{k}}}, \quad (8)$$

where $\epsilon_{\mathbf{k}}=2t\cos(|\mathbf{k}|)-\mu$ and $f(\epsilon)$ is the Fermi distribution function. Figure 4 shows $\chi(\mathbf{Q},\omega=0)$ as a function of the chemical potential μ for a finite system. The maxima of the CDW susceptibility occur for such $\mathbf{Q}$'s that both the energies in the denominator in Eq. (8) vanish, i.e., for $\epsilon_{\mathbf{k}}=0$ and $\mathbf{Q} =2\mathbf{k}$. In the case of an infinite system $\mathbf{k}$ changes continuously and the first equation has a solution for an arbitrary value of the chemical potential. Then, the maximum of the CDW susceptibility occurs for $\mathbf{Q}$ that satisfies the condition $\mu=2t\cos(|\mathbf{Q}|/2)$. On the other hand, for a finite system, $\mathbf{k}$ takes on discrete values and the maxima of the CDW susceptibility occur only for specific values of μ, i.e., when μ is equal to one of the energy levels. This feature is responsible for the CDW-induced plateaus in the *I-V* characteristics. In the case of noninteracting electrons the steps arise due to resonant tunneling through a multilevel quantum system. The steep sections occur when the successive energy levels are taking part in the charge transport. However, simultaneously the criterion discussed above for the onset of CDW is satisfied. As a result, the CDW gap opens and new plateaus occur in the middle of these steep sections.

But still there is a question concerning the degree of steepness of the sections that connect the plateaus. It determines the height of peaks in the differential conductance. The width of the one-particle energy levels is related to Γ. When the system is weakly coupled to the electrodes the
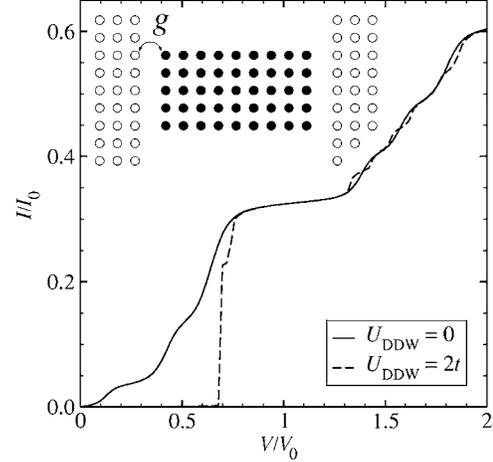
FIG. 5. Current-voltage characteristics of a 10×4 nanosystems coupled to the leads, as shown in the inset. Continuous and dashed lines show results obtained for $U_{\text{CDW}}=0$ and $2t$, respectively. We have neglected the energy dependence of $\hat{\Gamma}_{\alpha}(\omega)$ and adjusted the value of the hopping energy g in such a way that $[\hat{\Gamma}_{\alpha}(\omega)]_{ii} =0.1t\delta_{i\alpha}$ [see Eq. (5) for the details].

energy levels are very narrow and the *I-V* characteristic consists of sharp steps, provided the temperature is low enough. Increase of Γ smooths out these steps. It holds true both in the presence and in the absence of CDWs, which can be inferred from Figs. 1(a) and 1(b).

In the following we investigate the influence of the transverse dimension of the nanosystem. For that purpose we consider a nanowire of a finite width. In such a case the description of the coupling between the nanosystem and the leads becomes nontrivial. We assume a simple model in which leads are described by a two-dimensional (2D) lattice gas and the hopping between the leads and nanosystem is possible only perpendicularly to the edge of the nanosystem (see the inset in Fig. 5). Then, the nonvanishing elements of the matrices $\hat{\Gamma}_{L}(\omega)$ and $\hat{\Gamma}_{R}(\omega)$ can be calculated directly from the Eq. (5):

$$[\hat{\Gamma}_{\alpha}(\omega)]_{ij} = 2\pi\sum_{\mathbf{k}}|g|^2\delta_{i\alpha}\delta_{j\alpha}\cos(\mathbf{k}\cdot\mathbf{R}_{ij})\delta(\omega-\varepsilon_{\mathbf{k},\alpha}), \quad (9)$$

where g denotes the hopping amplitude and $\mathbf{R}_{ij}=\mathbf{R}_i-\mathbf{R}_j$. $\delta_{iR(L)}$ is equal to 1 if the site i is located at the right (left) edge of the nanosystem and vanishes otherwise.

Figure 5 shows the *I-V* characteristics for a four-site-wide and ten-site-long nanosystem calculated for $U_{\text{CDW}}=2t$ and 0. Contrary to the 1D case an important difference between the correlated and uncorrelated cases is visible only for low voltage. We have found that in this case there exists a commensurate CDW with the wave vector $\mathbf{Q}=(\pi,\pi)$. Increasing of V leads to a disappearance of the CDW ordering. There exist minor differences between both the characteristics for larger values of V. However, they appear irregularly and are much smaller than in the 1D case. Therefore, the voltage-induced incommensurate CDW seems to be an intrinsic feature only of the 1D systems. One may attribute this behavior to general properties of the density wave systems; namely, in the 2D

case the nesting of the Fermi surface plays a crucial role for stability of the CDW phase. The CDW wave vector connects the nested parts of the Fermi surface. For a square lattice with the nearest-neighbor hopping the Fermi surface is perfectly nested only in the half-filled case, which corresponds to the commensurate $\mathbf{Q}=(\pi,\pi)$. Other values of $\mathbf{Q}$ do not correspond to a perfectly nested Fermi surface. Therefore, an incommensurate CDW in 2D systems is usually less stable than in 1D cases. We believe that this property is responsible for the visibly different I-V characteristics of 1D and 2D systems.

IV. UNCONVENTIONAL CHARGE DENSITY WAVES

In the following we extend our analysis by taking into account unconventional density waves, where a condensation of electron-hole pairs with nonzero angular momentum occurs.[13] Such a state, with the angular momentum $l=2$, has recently been proposed as an explanation for the pseudogap phenomena in high-temperature superconductors.[14] In contrast to conventional density waves the charge is distributed uniformly over the whole system, but there occur orbital currents, i.e., the state breaks the time-reversal symmetry. This difference may be visible in the transport properties because of the interference between the transport and orbital currents. Recent developments in the fabrication techniques allow one to produce nanowires out of high-temperature superconductors.[20] The pseudogap is visible in these systems. Moreover, a discrete switching noise in the resistance of the nanowires has been observed in the pseudogap regime and explained in terms of the formation of the stripe phase. It suggests that interesting phenomena emerge in high-temperature superconductors, when one enters the meso- and nanoscales. One may also expect that these results may contribute to understanding of the pseudogap phenomenon. In particular, a question arises as to whether the results presented in Ref. 20 can be explained within the unconventional density wave scenario of the pseudogap.

In order to investigate this problem within the formalism introduced above, we have considered a system described by the Hamiltonian (1) with $U_{CDW}=0$. Figure 6 shows the resulting current-voltage characteristics obtained for $U_{DDW}=1.6t$ and 0. They are very similar to those of conventional 2D CDWs for low and sufficiently high voltages. In the first case, i.e., for low voltage, the energy gap does not allow for current flow and the system is insulating. In the opposite case, the applied voltage destroys both conventional and unconventional density waves. However, for unconventional density waves there exists also an intermediate regime, where the transport current is finite but the I-V characteristic significantly differs from the results obtained for the uncorrelated system ($U_{DDW}=0$). In this regime sharp steps in the I-V characteristic occur, indicating rapid changes of the orbital current distribution. Figure 7 shows the spatial distributions of the orbital currents Δ_i at various voltages, where Δ_i is given by

$$\Delta_i = \frac{1}{4}(W_{i,i+\hat{\mathbf{x}}} + W_{i,i-\hat{\mathbf{x}}} - W_{i,i+\hat{\mathbf{y}}} - W_{i,i-\hat{\mathbf{y}}}). \qquad (10)$$
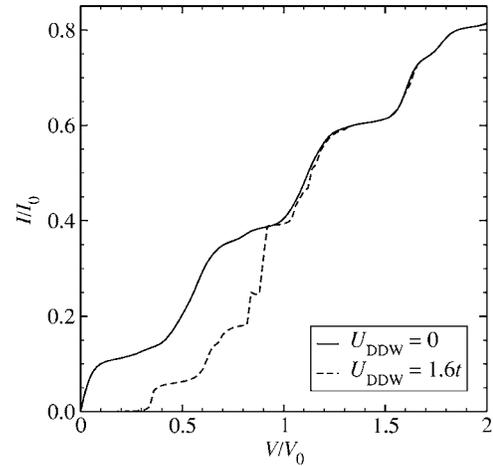
FIG. 6. Current-voltage characteristics of a 20×6 nanosystem coupled to the leads, as shown in the inset of Fig. 5. Continuous and dashed lines show results obtained for $U_{DDW}=0$ and $1.6t$, respectively. The remaining model parameters are the same as described in the caption of Fig. 5.

For a low voltage Δ_i is almost independent of the lattice site i, which indicates the uniform magnitude of the orbital currents. The sudden drop of Δ_i at the system edges originates from the reduced number of neighboring sites [see Eq. (10)]. Increase of V reduces the magnitude of the orbital currents. Additionally, this quantity becomes spatially modulated, as can be inferred from Fig. 7. The modulation is mostly visible in the longitudal direction. It is an almost periodic modulation, with the period decreasing with increasing V. This behavior is opposite to the previously discussed 1D conventional CDW, where the period of the charge modulation increases with V. There exist lines where Δ_i changes sign, which corresponds to reversed circulation of the orbital currents. The voltage-induced transitions between various distributions of Δ_i are accompanied by sharp steps in the I-V characteristic. Therefore, one could speculate that in larger systems such transitions may be responsible for the switching noise in the resistance of the nanowires in the pseudogap phase,[20] i.e., in the phase that could be described as an unconventional density wave state.[14]

V. DISCUSSION AND CONCLUDING REMARKS

In order to investigate the transport properties of nanosystems with charge density waves we have applied the formalism of nonequilibrium Keldysh Green's functions. Both conventional and unconventional states have been considered. Most of the already published results concern the sliding CDW, where it is assumed *a priori* whether the density waves are commensurate or not. It has previously been shown that the transport properties of commensurate and incommensurate CDW systems are different. On the other hand, it is known that commensurability of an isolated 1D CDW system depends on the position of the Fermi level, or equivalently on the occupation number. In the case of transport through a nanosystem, its properties are determined by the chemical potentials of the left and right electrodes, which
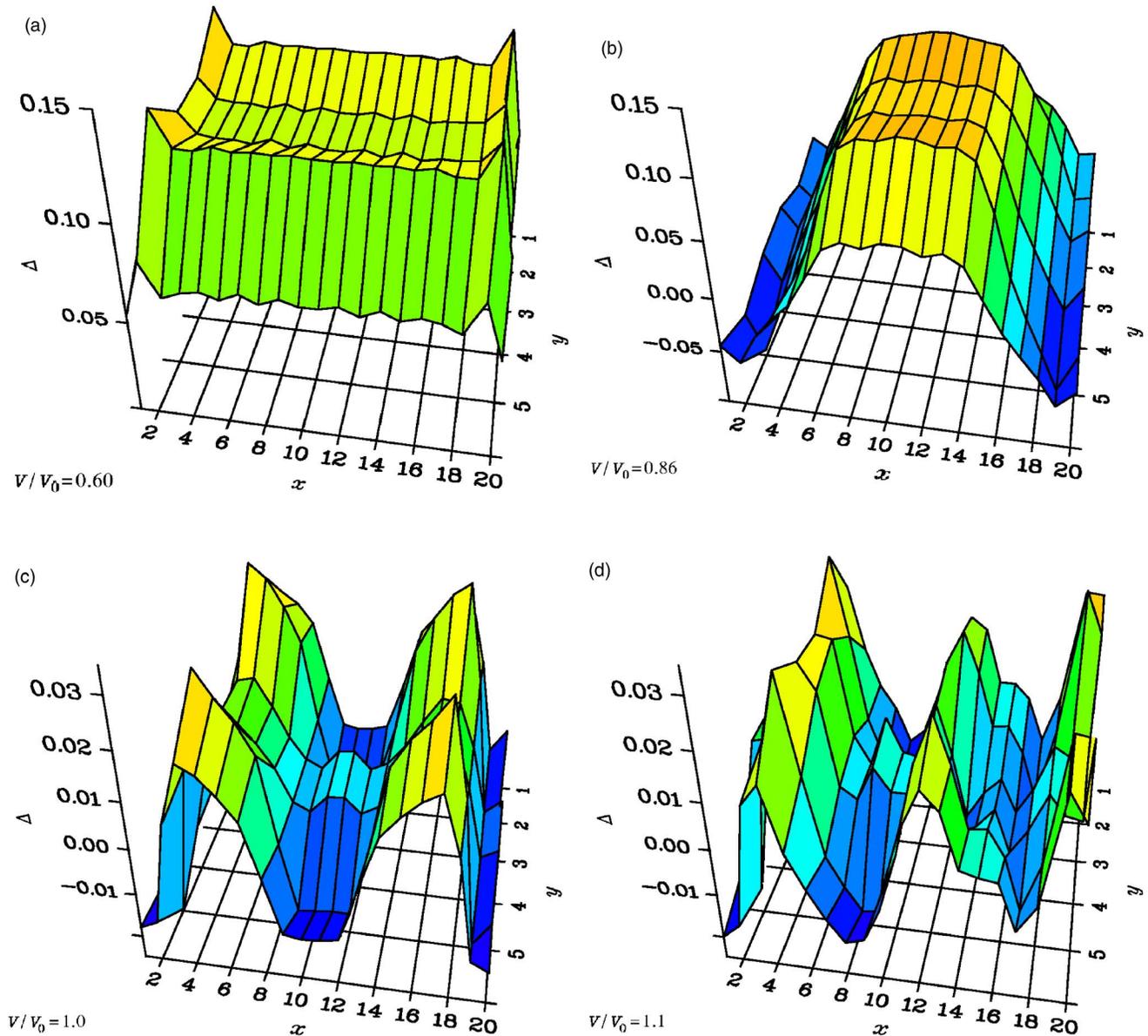
FIG. 7. (Color online) Spatial distribution of the orbital currents Δ_i. The voltage is indicated explicitly in the figure, whereas the remaining model parameters are the same as in Fig. 6.

are shifted by the applied voltage. We have shown that in the case of a 1D CDW system the commensurability changes with the voltage, whereas the average concentration of electrons remains unchanged. These CDW states occur only for specific, periodically distributed ranges of the voltage. The number of the allowed values of the **Q** vector increases with increase of the length of the system. Therefore, we expect that for a sufficiently long nanowire **Q** should linearly decrease with increasing applied voltage. We have shown that the applied voltage affects also the unconventional density waves. In particular, it leads to spatial modulation of the orbital currents, especially in the longitudal direction. It is a remnant of the voltage-dependent charge modulation that occurs in a 1D system with a conventional CDW. However, in contrast to the CDW case the period of this modulation decreases with increase of V. The difference between the I-V

characteristics obtained for a 2D nanosystem with conventional and unconventional CDWs is attributed to the interference between the transport and orbital currents that occurs in the latter case.

To summarize, we have shown that the properties of nanosystems with conventional and unconventional density waves strongly depend on the applied voltage. The discussed mechanism should be taken into account also in an analysis based on the sliding CDW mechanism, since the transport properties depend on the commensurability.

ACKNOWLEDGMENT

[1] J. Chen, M. A. Reed, A. M. Rawlett, and J. M. Tour, Science **286**, 1550 (1999).

[2] H. Park, J. Park, A. K. L. Lim, E. H. Anderson, A. P. Alivisatos, and P. L. McEuen, Nature (London) **407**, 57 (2000).

[3] Z. J. Donhauser, B. A. Mantooth, K. F. Kelly, L. A. Bumm, J. D. Monnell, J. J. Stapleton, D. W. Price, Jr., A. M. Rawlett, D. L. Allara, J. M. Tour, and P. S. Weiss, Science **292**, 2303 (2001).

[4] D. I. Gittins, D. Bethell, D. J. Schiffrin, and R. J. Nichols, Nature (London) **408**, 67 (2000).

[5] H. S. J. van der Zent, N. Marković, and E. Slot, Usp. Fiz. Nauk **171**, 61 (2001).

[6] O. C. Mantel, C. A. W. Bal, C. Langezaal, C. Dekker, and H. S. J. van der Zant, Phys. Rev. B **60**, 5287 (1999).

[7] K. L. Ringland, A. C. Finnefrock, Y. Li, J. D. Brock, S. G. Lemay, and R. E. Thorne, Phys. Rev. B **61**, 4405 (2000).

[8] L. E. Oxman, E. R. Mucciolo, and I. V. Krive, Phys. Rev. B **61**, 4603 (2000); B. Rejaei and G. E. W. Bauer, *ibid.* **54**, 8487 (1996).

[9] I. V. Krive, A. S. Rozhavsky, E. R. Mucciolo, and L. E. Oxman, Phys. Rev. B **61**, 12835 (2000).

[10] T. Kostyrko and B. R. Bułka, Phys. Rev. B **67**, 205331 (2003).

[11] E. G. Emberly and G. Kirczenow, Phys. Rev. B **64**, 125318 (2001).

[12] C. P. Collier, G. Mattersteig, E. W. Wong, Y. Luo, K. Beverly, J. Sampaio, F. M. Raymo, J. F. Stoddart, and J. R. Heath, Science **289**, 1172 (2000).

[13] C. Nayak, Phys. Rev. B **62**, 4880 (2000).

[14] S. Chakravarty, R. B. Laughlin, D. K. Morr, and C. Nayak, Phys. Rev. B **63**, 094503 (2001); S. Tewari, H. Y. Kee, C. Nayak, and S. Chakravarty, *ibid.* **64**, 224516 (2001).

[15] M. M. Maśka and M. Mierzejewski, Phys. Rev. B **68**, 024513 (2003).

[16] K. Maki, B. Dóra, M. Kartsovnik, A. Virosztek, B. Korin-Hamzić, and M. Basletić, Phys. Rev. Lett. **90**, 256402 (2003).

[17] J. X. Zhu, W. Kim, C. S. Ting, and J. P. Carbotte, Phys. Rev. Lett. **87**, 197001 (2001).

[18] K. Czajka, M. M. Maśka, M. Mierzejewski, and Ż. Śledź, Phys. Rev. B **72**, 035320 (2005).

[19] The transport current is often expressed in units of $2e\Gamma/h$. In the following, we investigate also a 2D case, when the coupling between the electrodes and nanosystem is described by the matrix $\hat{\Gamma}_{ij}$. In order to use the same units in 1D and 2D cases, instead of Γ we make use of the hopping integral t.

[20] J. A. Bonetti, D. S. Caplan, D. J. Van Harlingen, and M. B. Weissman, Phys. Rev. Lett. **93**, 087002 (2004).